World Engineering & Applied Sciences Journal 10 (1): 13-22, 2019
ISSN 2079-2204

DOI: 10.5829/idosi.weasj.2019.13.22

Conjugate Analysis of Galvanized Steel Corrosion Rate Using Operational Influences of Immersion-Point pH and Exposure Time in Sea Water Environment

[1]P.C. Nwosu, [1]P.C. Okoye, [2]O.K. Orieke, [1]S.J. Olagunju,
[1]K.A. Azodoh, [1]J.U. Onwuzuruigbo and [3]C. I. Nwoye

[1]Department of Mechanical Engineering, Federal Polytechnic, Nekede, Owerri, Nigeria
[2]Department of Mechanical Engineering, Federal University of Technology, Owerri, Nigeria
[3]Department of Metallurgical and Materials Engineering, Nnamdi Azikiwe University, State, Anambra State, Nigeria

Abstract: The paper presents an analysis of galvanized steel corrosion rate in sea water environment using operational influences of immersion-point pH (pH of stagnant sea water trapped in holes and grooves of galvanized steel made structures or equipment) and exposure time. Corrosion rate dependence of galvanized steel on both the immersion-point pH and exposure time was evaluated. Analysis of the surface structures of corroded galvanized steel were carried out to evaluate the phase distribution morphology. Response coefficient of the steel corrosion rate to the combined influence of exposure time ϑ and immersion-point pH γ were evaluated to ascertain the reliability of the highlighted dependence. The corrosion rate of the galvanized steel decreased with increase in the exposure time and immersion-point pH due to the formation of $(ZnOH)_2$. SEM analysis of the surface structure of the corroded steel revealed that the adherent and compact nature of the white rust layers absorbed on the zinc surface affected the level of corrosion attacks on the zinc and invariably on the steel structure. This was because oxidation of zinc due to oxygen inflow was affected by the white rust compact and adherent nature. A two-factorial model was derived, validated and used for the predictive evaluation of the galvanized steel corrosion rate. The validity of the model;

$$\zeta = -3.5\ x\ 10^{-4}\vartheta - 10^{-5}\gamma + 8.428\ x\ 10^{-5}$$

was rooted on the core model expression $\zeta + 3.5 \times 10^{-4}\ \vartheta = - 10^{-5}\ \gamma + 8.428 \times 10^{-5}$ where both sides of the expression are correspondingly approximately equal. The corrosion penetration depth per as obtained from experiment, derived model and regression model-predicted results were 1.84×10^{-7}, 2.07×10^{-7} and 1.98×10^{-7} mm respectively. Standard errors incurred in predicting the corrosion rate for each value of the exposure time & immersion-point pH considered as obtained from experiment, derived model and regression model-predicted results were 1.468×10^{-6}, 1.211×10^{-8} and 1.348×10^{-8} & 1.472×10^{-6}, 2.739×10^{-9} and 3.38×10^{-9} % respectively. Deviational analysis indicates that the maximum deviation of model-predicted corrosion rate from the experimental results was less than 15%. This translated into over 85% operational confidence and response level for the derived model as well as over 0.85 reliability response coefficient of corrosion rate to the collective operational contributions of exposure time and immersion-point pH in the sea environment.

Key words: Analysis · Galvanized Steel Corrosion Rate · Immersion-Point Ph · Exposure Time · Sea Water Environment

INTRODUCTION

All over the world, galvanized steel is widely known and streamlined as an effective and economical material of construction for evaporative cooling systems. Galvanized steel consists of a thin coating of zinc fused to a steel substrate. This combination provides material that has the mechanical properties of steel enhanced with the corrosion resistance of zinc [1].

Corresponding Author: P.C. Nwosu, Department of Mechanical Engineering, Federal Polytechnic Nekede, Owerri, Nigeria.

Researchers [1] has shown that the nature of the corrosion product observed on the surface of galvanized steel, following its exposure in water environment is waxy and white. This is referred to as white rust. The scientists posited that white rust is a rapid, localized corrosion attack on zinc that usually appears as a voluminous white deposit. This rapid corrosion can completely remove zinc in a localized area with the resultant reduction in equipment life. Results from the research [1] revealed that if the white-rust corrosion product is kept wet it often feels waxy; if the corrosion product dries it usually feels hard and brittle. Observations made during the research also indicated that beneath the white deposit, there exists a localized area where the zinc has been attacked. In its early stages this area appears as a shallow pit.

A comparative study of the corrosion behavior of galvanized steel under 3.5wt % NaCl and chloride- free simulated rust layer (SRL) solution was investigated [2] using polarization curve and electrochemical impedance spectroscopy (EIS). The morphology, organization and chemical properties of the rust layer were detected by scanning electron microscopy (SEM), X-ray diffraction (XRD) and energy dispersive spectroscopy (EDS). The results indicated that the rust layer could inhibit the corrosion of galvanized steel in chloride-free SRL solution, both of the resistance of rust layer (Rf) and charge transfer resistance (Rct) increased with the increase of immersion time. However, non-uniform corrosion occurred on the galvanized steel in the SRL solution containing 3.5wt% NaCl, the rust layer absorbed on the electrode was gradually destroyed under the erosion of Cl^- [2].

Recent studies [3-6] have evaluated the applicability of galvanized steel and found it useful in areas such as building, automotive body parts and water distribution systems because of its good resistance to environmental corrosion. The protection obtained by zinc coating is due to barrier and galvanic double protective effect [7, 8]. However, many cases of heavy damage of galvanized pipes and tanks have been reported as being due to corrosion processes in water hanging system, as clearly evidenced by the production of rust layer in those systems after an unexpectedly short lifetime [9].

Research findings [10-12] on atmospheric corrosion of galvanized steel have revealed that the composition of the rust layer on galvanized steel depends on the exposure conditions, type and level of the pollutants, as well as the number of the wet- dry cycles. The most abundant corrosion products in an unpolluted aqueous solution are ZnO and $Zn(OH)_2$ [13, 14]. The rust layer absorbed on the zinc coating surface affects corrosion- related processes, such as the mass transport of dissolved oxygen, the stability of the passive film and the hydration of the dissolved metal ions. Besides, the corrosion reactions under rust layer are not only simple reactions including metal anodic dissolution and oxygen reduction, but also complex corrosion process composed of multiple sub-processes involving rust redox reactions, mass transportation through rust, electric charges movement between interfaces, microorganism propagation in porous rust and some other complex corrosion processes [15-18].

It has been proposed [19] that zinc ion dissolved from the rust layer on galvanized steel preventing further corrosion of the steel substrate. The researcher demonstrated the contribution of the zinc-containing rust layer to the corrosion retardation for the Fe substrate, as well as the high sacrificial anode effect of the metallic zinc.

Investigations [20, 21] have been carried out on the dissolution and corrosion mechanism of high purity zinc in an aerated sulfate medium by using electrochemical impedance analysis and by modeling the process. There were three parallel paths of zinc dissolution and three absorbed intermediates (Zn^+_{ad}, Zn^{2+}_{ad} and $ZnOH_{ad}$) during the anodic dissolution process. Results of the investigation significantly revealed that both of the surface preparation conditions and the rust layer absorbed on the electrode surface would affect the balance between the competitive dissolution.

Past scientific discoveries [22-24] have indicated that the good corrosion resistance of zinc coating could be improved by alloying zinc with other metal (e.g. Co, Ni, Mn, Al). Some researchers have therefore suggested that the higher protective ability of these systems is due to the corrosion products, zinc hydroxide salts ($Zn(OH)_2$), that formed as a result of interaction with the corrosion medium [25].

It is strongly believed that the corrosion current and corrosion potential are sensitive to the zinc surface conditions as well as to the environment factors (pH of the solution, dissolved oxygen concentration, Cl^- ion concentration, temperature, etc). These factors have been related to the presence of oxidized species (oxide, hydroxide and carbonate) because of the contact with aqueous solution and to the contribution of the cathodic reduction of dissolved oxygen.

Proposed zinc dissolution mechanism [20] indicates that zinc dissolution in aqueous solution depends on the adsorbed intermediate species (Zn^+_{ad}, Zn^{2+}_{ad} and $ZnOH_{ad}$) as followed:

$$Zn \rightleftarrows Zn^{+}_{ad} + e \quad (1)$$

$$Zn^{+}_{ad} \rightarrow e + Zn^{2+}_{ad} \quad (2)$$

$$Zn + H_2O \rightarrow 1/2H_2 + ZnOH_{ad} \quad (3)$$

Therefore, the intermediates species adsorbed on the electrode surface play a "self-catalytic" role in the corrosion of zinc coating:

$$Zn^{+}_{ad} + Zn \rightarrow Zn^{2+}\,sol + Zn^{+}_{ad} + 2e \quad (4)$$

$$Zn^{2+}_{ad} \rightarrow Zn^{2+} \quad (5)$$

$$ZnOH_{ad} + Zn \rightarrow ZnOH_{ad} + Zn^{2+}sol + 2e \quad (6)$$

$$ZnOH_{ad} \rightarrow ZnOH^{+}\,sol + e \quad (7)$$

$$ZnOH^{+}\,sol \rightarrow Zn^{2+}\,sol + OH^{-} \quad (8)$$

The adsorbed species, such as Zn^{+}_{ad}, Zn^{2+}ad and $ZnOH_{ad}$, could be the reason for the low frequency inductive loop.

The aim of this research is focused on the conjugate analysis of galvanized steel corrosion rate using operational influences of immersion-point pH and exposure time in natural sea water. A model will be derived, validated and used for the analysis. Galvanized steel made structures and equipment used for sea water evaporating system are known to have series of holes and grooves which entrap water. And so, the corrosion rates of these areas could be analyzed using these operational influences by substituting them into the derived model.

MATERIALS AND METHODS

Materials used for the experiment are galvanized steel pipes obtained from oil fields in Port Harcourt, Nigeria. The other materials used were acetone, sodium chloride, distilled water, beakers and measuring cylinders. The equipment used were drilling machine, analytical digital weighing machine.

Specimen Preparation and Experimentation: The galvanized steel pipes collected for the purpose of this work were cleaned using 0.5M picric acid to remove any existing trace of rust. These pipes were then washed in running water, distilled water and acetone before air-drying at room temperature. The dried steel pipes were cut into test samples of known dimensions and weighed.

Fig. 1: Galvanized steel pipe

Fig. 2: Corroded pieces of galvanized steel cut and exposed to sea water environment

Each sample piece was drilled with 5mm drill bit to provide hole for the suspension of the strings and submersion of the sample in the sea water.

The method adopted for this phase of the research is the weight loss technique. The test pieces were weighed and exposed to 200cm^3 of sea water contained in a beaker for 250 hrs after which they were withdrawn.The pH of the sea water was measured as each test piece was withdrawn. The withdrawn test pieces were washed with distilled water, cleaned with acetone and dried in open air before weighing to determine the final weight. The experiment was repeated for 270, 290, 300 as well as 400hrs exposure time and the corresponding sea water pH measured.

RESULTS AND DISCUSSION

Surface Structural Analysis of Corroded and Un-corroded Galvanized Steel: The corrosion processes of the galvanized steel changed differently under the same sea water Cl^-concentration. Fig. 3 shows the SEM images at different sampling time intervals. Fig. 3 (a) presented the SEM images of the as-received sample of galvanized steel before immersion in sea water.

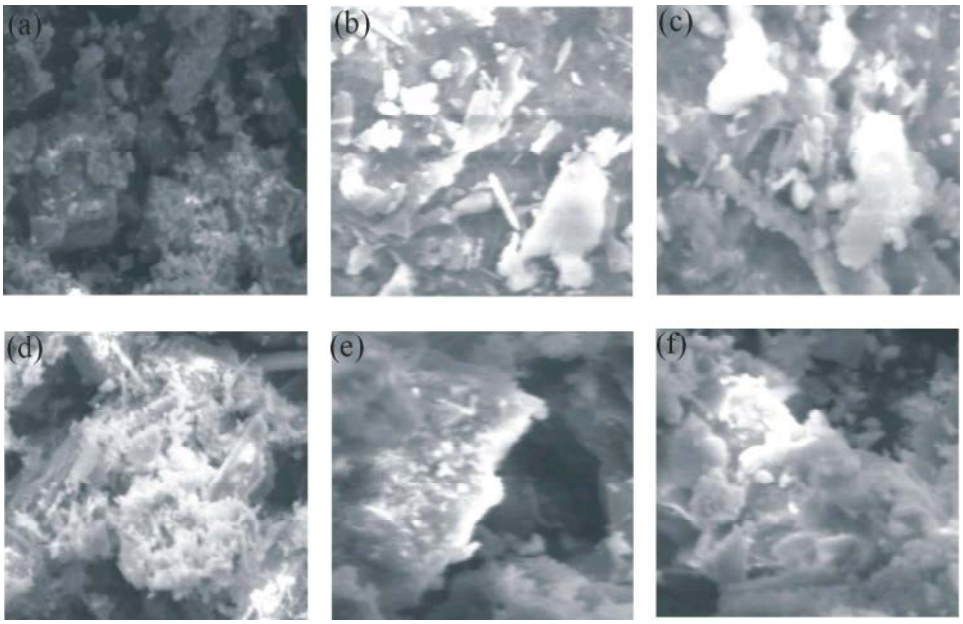

Fig. 3: The SEM images of galvanized steel in sea water environment for different exposure times: (a) before immersion; (b) 250 hrs; (c) 270 hrs; (d) 290 hrs, (e) 300 hrs; (f) 400 hrs (50μm)

This image of (un-corroded steel) presented here was for comparison with those of corroded samples. Evidently, the zinc coatings were compact, smooth and completely covered the substrate surface, no corrosion was found before the immersion of the test piece. Loose white rust and corrosion products were absorbed on the zinc surface after 250 hrs (Fig. 3(b)); as time continued elapsing, pitting corrosion occurred obviously on the galvanized steel after 270 hrs (Fig.3 (c)). This is shown by the white spots in the image, since they designate localized corrosion attack on the zinc covering in the steel [1]. These results further supported the assumption of the oxygen diffusion control step. With time, the rust layer absorbed on the zinc coating was gradually damaged under the erosion of Cl^-. However, lots of needle-like white rust layers (Fig. 3(d)) were adherent and compactly absorbed on the zinc surface and so reduced pitting corrosion was observed on the zinc coating after 290 hrs. This indicates drop in corrosion attack. Also Fig. 3(e) shows a reduction in the white waxy rust at 300 hrs (compared with other exposure times) due to decrease in the inflow of oxygen. This resulted from the compact nature of the formed protective film at this particular exposure time. Therefore the associated corrosion attack also decreased. At an exposure time of 400 hrs (Fig. 3 (f)), the white rust deposit further deceased due to much significant decrease in the inflow of oxygen, resulting from an increased compact nature of the formed protective film. This resulted to much decrease in the corrosion attack on the galvanized steel.

Table 1: Variation of corrosion rate ζ of galvanized steel with its exposure time ϑ (hr) and immersion-point pH γ

(ζ) (mm/yr)	(γ)	(ϑ) (hr)
1.301 x10^{-5}	6.00	250
1.274 x10^{-5}	6.08	270
1.248 x10^{-5}	6.16	290
1.236 x10^{-5}	6.20	300
2.321 x10^{-6}	6.60	400

Table 2: Variation of corrosion rate ζ of galvanized steel with its exposure time ϑ (yr) and immersion -point pH γ

(ζ) (mm/yr)	(γ)	(ϑ) (yr)
1.301 x10^{-5}	6.00	0.0285
1.274 x10^{-5}	6.08	0.0308
1.248 x10^{-5}	6.16	0.0331
1.236 x10^{-5}	6.20	0.0342
2.321 x10^{-6}	6.60	0.0457

Variation of Corrosion Rates with Immersion-point Ph and Exposure Time: Tables 1 and 2 present similar results except the conversion of alloy exposure time from hour (hr) to year (yr). Tables 1 and 2 show that the corrosion rate of the galvanized steel decreases with increase in the immersion-point pH and exposure time. It was believed that the protective film on the zinc grew and its coherency enhanced with increased exposure time. Based on the foregoing, the corrosion rate dropped due to decrease in oxygen inflow through the zinc coating.

$$Zn(s) + 1/2O_2 + H_2O\ Zn(OH)_2\ ZnO + H_2O \quad (9)$$

Table 3: Variation of $\zeta + 3.5 \times 10^{-4}\ \vartheta$ with $- 10^{-5}\ \gamma + 8.428 \times 10^{-5}$

$\zeta + 3.5 \times 10^{-4}\ \vartheta$	$- 10^{-5}\ \gamma + 8.428 \times 10^{-5}$
2.299×10^{-5}	2.428×10^{-5}
2.352×10^{-5}	2.348×10^{-5}
2.407×10^{-5}	2.268×10^{-5}
2.433×10^{-5}	2.228×10^{-5}
1.832×10^{-5}	1.828×10^{-5}

Decrease in the corrosion rate of galvanized steel with increase in immersion-point pH stems on the formation of $Zn(OH)_2$ (which reversibly gives $ZnO + H_2O$) from the reaction between OH^- and Zn^{2+}. This reaction actually brought about the initial rust. Therefore presence of $Zn(OH)_2$ or ZnO in aqueous solution (around the immersed galvanized steel) during the corrosion process increases the immersion-point pH and invariably the corrosion resistance in line with past findings [26]. OH^- was formed as result of oxygen reduction at the cathodic zone as shown in the equation:

$$½\ O_2 + H_2O + 2e\ 2OH^- \quad (10)$$

Computational analysis of generated experimental data shown in Table 2, gave rise to Table 3 which indicate that;

$$\zeta + K\ \vartheta = - N\ \gamma + S \quad (11)$$

Introducing the values of K, N and S into equation (11) reduces it to;

$$\zeta + 3.5 \times 10^{-4}\ \vartheta = - 10^{-5}\ \gamma + 8.428 \times 10^{-5} \quad (12)$$

$$\zeta = - 3.5 \times 10^{-4}\ \vartheta - 10^{-5}\ \gamma + 8.428 \times 10^{-5} \quad (13)$$

where
K = 0.00035, N = 0.00001, S= $8.428 \times 10^{-5}$are empirical constants (determined using C-NIKBRAN [27]
(ζ) = Corrosion rate (mm/yr)
(ϑ) = Exposure time (yr)
(γ) = Immersion-point pH (pH of sea water trapped in holes and grooves of galvanized steel made structures or equipment)

The derived model is equation (13). Computational analysis of Table 2 gave rise to Table 3. The derived model is two-factorial in nature since it is composed of two input process factors: exposure time and immersion-point pH. This implies that the predicted corrosion rate of galvanized steel in the sea water environment is dependent on just two factors: exposure time and galvanized steel immersion-point pH.

Boundary and Initial Conditions: Consider short cylindrically shaped galvanized steel exposed to sea water environment, interacting with some corrosion-induced agents. The sea water is assumed to be affected by unwanted dissolved gases. Range of exposure time considered: 250-400 hrs (0.0285-0.0457yrs), range of galvanized steel immersion point-pH considered: 6.0-6.6.

The boundary conditions are: aerobic environment for zinc coating (covering galvanized steel) oxidation (since the atmosphere contains oxygen. At the bottom of the exposed steel, a zero gradient for the gas scalar are assumed. The exposed steel is stationary. The sides of the solid are taken to be symmetries.

Model Validity: The validity of the model is strongly rooted on equation (12) (core model equation) where both sides of the equation are correspondingly approximately equal. Table 3 also agrees with equation (12) following the values of $\zeta + 3.5 \times 10^{-4}\ \vartheta$ and $- 10^{-5}\ \gamma + 8.428 \times 10^{-5}$ evaluated from the experimental results in Table 1. Furthermore, the derived model was validated by comparing the corrosion rate predicted by the model and that obtained from the experiment. This was done using various analytical techniques.

Statistical Analysis:
Standard Error (STEYX): The standard errors incurred in predicting the galvanized steel corrosion rate for each value of exposure time & immersion-point pH considered as obtained from experiment and derived model were 1.468×10^{-6} and 1.211×10^{-8}& 1.472×10^{-6} and 2.739×10^{-9}% respectively. The standard error was evaluated using Microsoft Excel version 2003.

Correlation: The correlation coefficient between galvanized steel corrosion rate and exposure time & immersion-point pH were evaluated (using Microsoft Excel Version 2003) from results of the experiment and derived model. These evaluations were based on the coefficients of determination R^2 shown in Figs. 4-7.

$$R = \downarrow R^2 \quad (14)$$

The evaluated correlations are shown in Tables 4 and 5. These evaluated results indicate that the derived model predictions are significantly reliable and hence valid considering its proximate agreement with results from actual experiment.

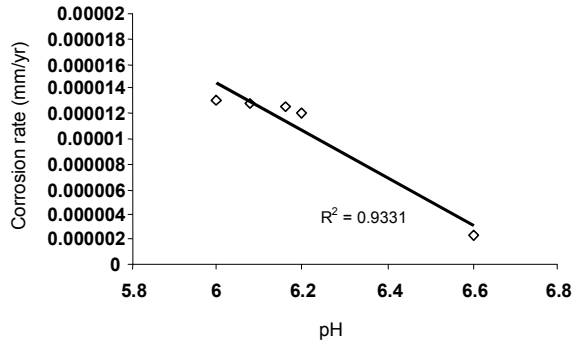

Fig. 4: Coefficient of determination between galvanized steel corrosion rate and immersion-point pH as obtained from the experiment

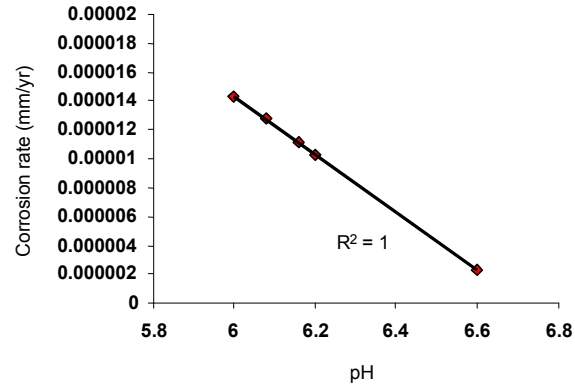

Fig. 5: Coefficient of determination between galvanized steel corrosion rate and immersion-point pH as predicted by derived model.

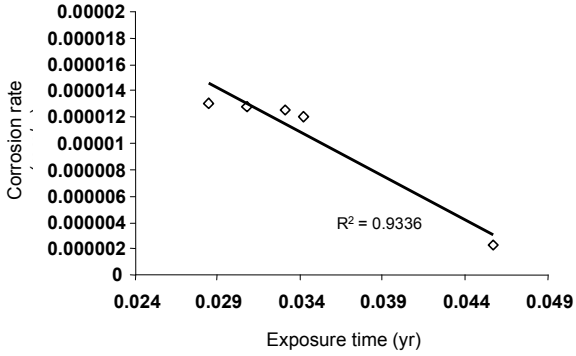

Fig. 6: Coefficient of determination between galvanized steel corrosion rate and exposure time as obtained from the experiment

Table 4: Comparison of the correlations between corrosion rate and exposure time as evaluated from experimental (ExD) and derived model (MoD) predicted results

	Based on exposure time	
Analysis	ExD	D-Model
CORREL	0.9662	1.0000

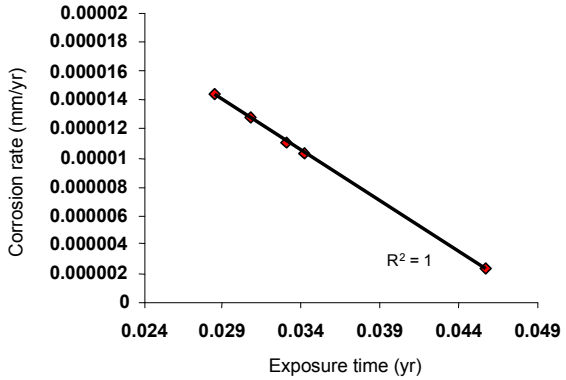

Fig. 7: Coefficient of determination between galvanized steel corrosion rate and exposure time as predicted by derived model

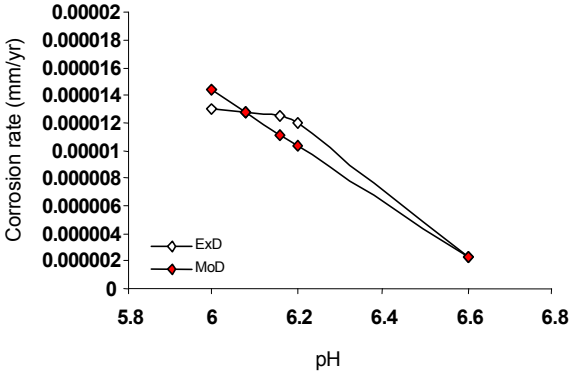

Fig. 8: Comparison of the galvanized steel corrosion rates (relative to immersion-point pH) as obtained from experiment and derived model.

Table 5: Comparison of the correlations between corrosion rate and immersion-point pH and as evaluated from experimental and derived model predicted results

	Based on immersion-point pH	
Analysis	ExD	D-Model
CORREL	0.9660	1.0000

Graphical Analysis: Graphical analysis of Figs. 8 and 9 shows very close alignment of the curves from derived model and experiment. It is strongly believed that the degree of alignment of these curves is indicative of the proximate agreement between ExD and MoD predicted results.

Comparison of Derived Model with Standard Model: The validity of the derived model was also verified through application of the regression model (ReG) (Least Square Method using Excel version 2003) in predicting the trend of the experimental results. Comparative analysis of Figs. 10 and 11 shows closely

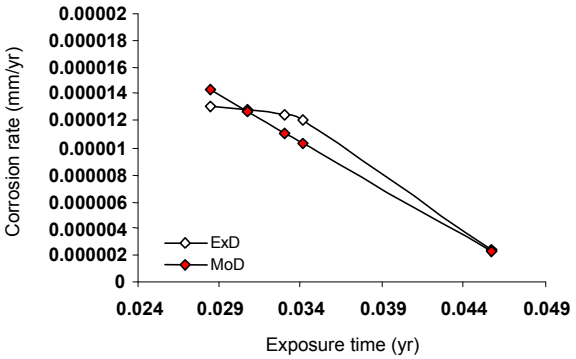

Fig. 9: Comparison of the galvanized steel corrosion rates (relative to exposure time) as obtained from experiment and derived model.

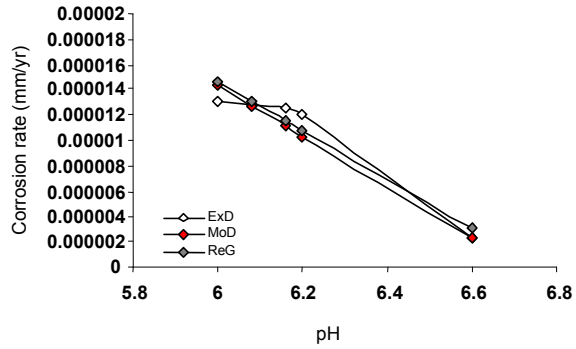

Fig. 10: Comparison of the galvanized steel corrosion rates (relative to immersion-point pH) as obtained from experiment, derived model and regression model

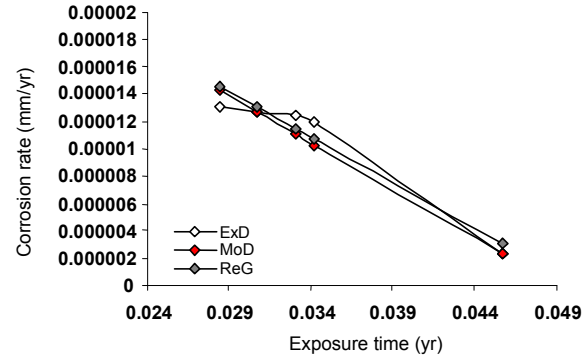

Fig. 11: Comparison of the galvanized steel corrosion rates (relative to exposure time) as obtained from experiment, derived model and regression model

aligned curves of corrosion rates, which precisely translated into significantly similar trend of data point's distribution for experimental (ExD), derived model (MoD) and regression model-predicted (ReG) results of corrosion rates.

Also, the calculated correlations (from Figs. 10 and 11) between galvanized steel corrosion rates and exposure time & immersion-point pH for results obtained from regression model were 1.0000 & 1.0000 respectively. These values are in proximate agreement with both experimental and derived model-predicted results. The standard errors incurred in predicting steel corrosion rates for each value of exposure time & immersion-point pH considered as obtained from regression model were 1.348 x 10^{-8} and 3.38 x 10^{-9} % respectively.

Computational Analysis: Computational analysis of the experimental and model-predicted corrosion penetration depth was carried out to ascertain the degree of validity of the derived model. This was done by comparing the corrosion penetration depth obtained by calculation, using experimental and model-predicted results.

Corrosion penetration depth in galvanized steel during the period of exposure in sea water environment ζ_S (mm) was calculated from the equation;

$$\zeta_S = \zeta \div \vartheta \tag{15}$$

Rewritten as

$$\zeta_S = \Delta\zeta \div \Delta\vartheta \tag{16}$$

Equation (16) is detailed as

$$\zeta_S = (\zeta_2 - \zeta_1) \div (\vartheta_2 - \vartheta_1) \tag{17}$$

where
$\Delta\zeta$ = Change in the corrosion rates (ζ_2 - ζ_1) at two Different exposure times ϑ_2, ϑ_1
$\Delta\vartheta$ = Change in the exposure times ϑ_2, ϑ_1

Considering the points (0.0285, 1.3x10^{-5}) & (0.0457, 2.3x10^{-6}),(0.0285,1.43x10^{-5}) & (0.0457, 2.29 x 10^{-6}) and (0.0285, 1.457 x 10^{-5}) & (0.0457, 3.04 x 10^{-6}) as shown in Fig. 11, designating them as (ζ_1, ϑ_1) & (ζ_2, ϑ_2) for experimental, derived model and regression model-predicted results respectively and then substituting them into equation (17), gives negative slopes: - 1.84 x 10^{-7}, - 2.07 x 10^{-7} and - 1.98 x 10^{-7} mm as their corrosion penetration depth respectively. For real practical purposes, only the magnitude of these values are considered as the ideal corrosion penetration depth. The negative sign simply shows that the corrosion rate

depicts an inverse relationship with the exposure time. Based on the foregoing, the corrosion penetration depth in galvanized steel (exposed to sea water environment) as obtained from experimental, derived model and regression model-predicted results are 1.84×10^{-7}, 2.07×10^{-7} and 1.98×10^{-7} mm respectively.

Deviational Analysis: Comparative analysis of the corrosion rates precisely obtained from experiment and derived model shows that the model-predicted values deviated from experimental results. This was attributed to the fact that the effects of the surface properties of the galvanized steel which played vital roles during the corrosion process were not considered during the model formulation. This necessitated the introduction of correction factor, to bring the model-predicted corrosion rate to those of the corresponding experimental values.

The deviation Dv, of model-predicted corrosion rate from the corresponding experimental result was given by

$$Dv = \frac{(\zeta_{MoD} - \zeta_{ExD})}{\zeta_{ExD}} \times 100 \quad (18)$$

where

ζ_{ExD} and ζ_{MoD} are corrosion rates evaluated from experiment and derived model respectively.

Figs. 12 and 13 show that the least and highest magnitudes of deviation of the model-predicted corrosion rate (from the corresponding experimental values) are – 0.31 and – 14.17%.

It could be seen from Figs. 12 and 13 that these deviations correspond to corrosion rates: $1.27 \times 10^{-5}$and 1.03×10^{-5}mm/yr, exposure times: 0.0308 and 0.0342 yrs as well as galvanized steel immersion pH: 6.08 and 6.2 respectively.

Comparative analysis of Figs. 12 and 13 also shows that the maximum deviation of model-predicted corrosion rate from the experimental results was less than 15%. This translated into over 85% operational confidence and response level for the derived model as well as over 0.85 reliability response coefficient of corrosion rate to the collective operational contributions of the exposure time and galvanized steel immersion-point pH (under service) in the sea water environment.

Correction factor, Cf to the model-predicted results was given by

$$Cf = - \frac{(\zeta_{MoD} - \zeta_{ExD})}{\zeta_{ExD}} \times 100 \quad (19)$$

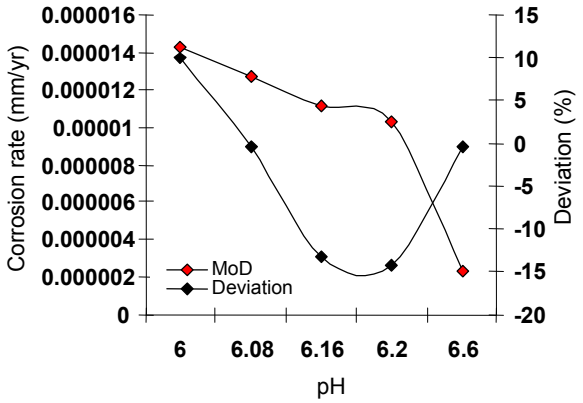

Fig. 12: Variation of model-predicted corrosion rate with associated deviation from experimental results (relative to immersion-point pH)

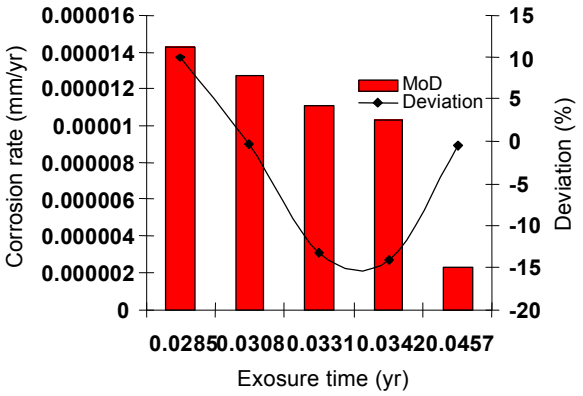

Fig. 13: Variation of model-predicted corrosion rate with associated deviation from experimental results (relative to exposure time)

Analysis of Table 6 in comparison with Figs. 12 and 13 indicates that the evaluated correction factors are negative of the deviation as shown in equations (18) and (19).

The correction factor took care of the negligence of operational contributions of the effects of surface properties of the galvanized steel which actually affected the corrosion process. The model predicted results deviated from those of the experiment because these contributions were not considered during the model formulation. Introduction of the corresponding values of Cf from equation (19) into the model gives exactly the corresponding experimental corrosion rate

Table 6 shows that the least and highest magnitudes of correction factor to the model-predicted corrosion rate are + 0.31 and + 1417%. Since correction factor is the negative of deviation (equations (12) and (13)), Table 6, Figs. 10 and 11 indicate that these correction factors correspond to corrosion rates:

Table 6: Variation of correction factor with exposure time and immersion-point pH

(ϑ) (yr)	(γ)	Cf (%)
0.0285	6.00	-10.00
0.0308	6.08	+ 0.31
0.0331	6.16	+13.28
0.0342	6.20	+14.17
0.0457	6.60	+ 0.43

1.27×10^{-5} and 1.03×10^{-5} mm/yr, exposure times: 0.0308 and 0.0342 yrs as well as galvanized steel immersion pH: 6.08 and 6.2 respectively.

It is important to state that the deviation of model predicted results from that of the experiment is just the magnitude of the value. The associated sign preceding the value signifies that the deviation is a deficit (negative sign) or surplus (positive sign).

CONCLUSION

The applicability of the operational influences of immersion-point pH and exposure time in studying the corrosion of galvanized steel in sea water environment has been ascertained. The corrosion rate of the galvanized steel decreased with increase in the exposure time and immersion-point pH due to the formation of $(ZnOH)_2$. SEM analysis of the surface structure of the corroded steel revealed that the adherent and compact nature of the white rust layers absorbed on the zinc surface affected the level of corrosion attacks on the zinc and invariably on the steel structure. Oxidation of zinc due to oxygen inflow was affected by the white rust compact and adherent nature. A two-factorial model was derived, validated and used for the predictive evaluation of the galvanized steel corrosion rate. The validity of the model was rooted on the core model expression $\zeta + 3.5 \times 10^{-4}\ \vartheta = - 10^{-5}\ \gamma + 8.428 \times 10^{-5}$ where both sides of the expression are correspondingly approximately equal. The corrosion penetration depth obtained from experiment, derived model and regression model-predicted results were 1.84×10^{-7}, 2.07×10^{-7} and 1.98×10^{-7} mm respectively. Standard errors incurred in predicting the corrosion rate for each value of the exposure time & immersion-point pH considered as obtained from experiment, derived model and regression model-predicted results were 1.468×10^{-6}, 1.211×10^{-8} and 1.348×10^{-8} & 1.472×10^{-6}, 2.739×10^{-9} and 3.38×10^{-9} % respectively. Deviational analysis indicates that the maximum deviation of model-predicted corrosion rate from the experimental results was less than 15%. This translated into over 85% operational confidence and response level for the derived model as well as over 0.85 reliability response coefficient of corrosion rate to the collective operational contributions of exposure time and immersion-point pH in the sea environment.

REFERENCES

1. Engineering Bulletin (Evapco), 2009. White Rust on Galvanized Sheet, No. #34A.
2. Huyuan, S., L. Shuan and S. Lijuan, 2013. A Comparative Study on the Corrosion of Galvanized Steel under Simulated Rust Layer Solution with and without 3.5wt%NaCl Int. J. Electrochem. Sci., 8: 3494-3509.
3. El-Sayed, M., A.A. Sherif, B. Almajid, A. K.Bairamov and A. Eissa, 2012. Int. J. Electrochem. Sci., 7: 2796-2810.
4. Yadav, A.P., H. Katayama, K. Noda, H. Masuda, A. Nishikata and T. Tsuru, 2007. Electrochem. Acta., 52: 3121-3129.
5. Amin, M.A., H.H. Hassan and S.A. Rehim, 2008. Electrochem. Acta., 53: 2600-2609.
6. Lin, B.L., J.T. Lu and G. Kong, 2008. Corros. Sci., 4: 962-967.
7. Bajat, J.B., S. Stankovic, B.M. Jokic and S.I. Stevanovic, 2010. Surf. Coat. Technol., 204: 2745-2753.
8. Kartsonakis, I.A., A.C. Balaskas, E.P. Koumoulos, C. A. Charitidis and G.C. Kordas, 2012. Corros. Sci., 57: 30-41.
9. Zhang, X.G., 2005. Corrosion of zinc and zinc alloys, Corrosion: Materials, ASM Handbook, pp: 402-406.
10. Zapponi, M., T. Perez, C. Ramos and C. Saragovi, 2005. Corros. Sci., 47: 923-936.
11. Azmat, N.S., K.D. Ralston, B.C. Muddle and I.S. Cole, 2011. Corros. Sci., 53: 1604-1615.
12. Yadav, A.P., A. Nishikata and T. Tsuru, 2004. Corros. Sci., 46: 169-181.
13. Mokaddem, M., P. Volovitch and K.C. Ogle, 2010. Electrochem. Acta., 55: 7867-7875.
14. Vu, T.N., M. Mokaddem, P. Volovitch and K. Ogle, 2012. Electrochem. Acta., 74: 130-138.
15. Zou, Y., J. Wang and Y.Y. Zheng, 2011. Corros. Sci., 53: 208-216.
16. Daun, J.Z., S.R. Wu, X.J. Zhang, G.Q. Huang, M. Du and B.R. Bao, 2008. Electrochim. Acta., 54: 22-28.
17. Bousselmi, L., C. Fiaud, B. Tribollets and E. Triki, 1997. Corros. Sci., 39: 1711-1724.
18. Yu, L., J.D. Duan, W. Zhao, Y.L. Huang and B.R. Hou, 2011. Electrochem. Acta., 56: 9041-9047.

19. Tsuru, T., 2010. Corros. Eng., 59: 321-329.
20. Cachet, C., F. Ganne, G. Maurin, J. Petitijean, V. Vivier and R. Wiart, 2001. Electrochem. Acta., 47: 509-518.
21. Catchet, C., F. Ganne, S. Joiret, G. Maurin, J. Petitijean, V. Vivier and R. Wiart, 2002. Electrochem. Acta., 47: 3409-3422.
22. Zhang, X., S.L. Russo, A. Miotello, L. Guzman, E. Cattaruzza, P.L. Bonora and L. Benedetti, 2001. Surf. Coat. Technol., 141: 187-193.
23. Volovitch, P., C. Allely and K. Ogle, 2009. Corros. Sci., 5: 1251-1562.
24. Boshkov, N., K. Petrov, S. Vitkova, S. Nemska and G. Raichevsky, 2002. Surf. Coat. Technol., 157: 171-178.
25. Oritz, Z.I., P. Diaz-Arista, Y. Meas, R. Ortega-Borges and G. Trejo, 2009. Corros. Sci., 51: 2703-2715.
26. Hamlaoui, Y., L. Tifouti and F. Pedraza, 2010. Corros. Sci., 52: 1883-1888.
27. Nwoye, C.I., 2008. C-NIKBRAN Data Analytical Memory (Software).